Highly accurate spatial mode generation using spatial cross modulation method for mode division multiplexing

Hiroki Sakuma[a*], Atsushi Okamoto[a], Atsushi Shibukawa[b], Yuta Goto[a], and Akihisa Tomita[a]
[a]Graduate School of Information Science and Technology, Hokkaido University,
Kita14-Nishi9, Kita-ku, Sapporo, 060-0814, Japan;
[b]Electrical Engineering, California Institute of Technology,
Pasadena, CA 91125, USA

ABSTRACT

We propose a spatial mode generation technology using spatial cross modulation (SCM) for mode division multiplexing (MDM). The most well-known method for generating arbitrary complex amplitude fields is to display an off-axis computer-generated hologram (CGH) on a spatial light modulator (SLM). However, in this method, a desired complex amplitude field is obtained with first order diffraction light. This critically lowers the light utilization efficiency. On the other hand, in the SCM, the desired complex field is provided with zeroth order diffraction light. For this reason, our technology can generate spatial modes with large light utilization efficiency in addition to high accuracy. In this study, first, a numerical simulation was performed to verify that the SCM is applicable for spatial mode generation. Next, we made a comparison from two view points of the coupling efficiency and the light utilization between our technology and the technology using an off-axis amplitude hologram as a representative complex amplitude generation method. The simulation results showed that our technology can achieve considerably high light utilization efficiency while maintaining the enough coupling efficiency comparable to the technology using an off-axis amplitude hologram. Finally, we performed an experiment on spatial modes generation using the SCM. Experimental results showed that our technology has the great potential to realize the spatial mode generation with high accuracy.

Keywords: optical fiber communication, mode division multiplexing, multi-mode fiber, spatial mode generation, computer holography, wavefront encoding, spatial light modulator, random diffuser

1. INTRODUCTION

Optical communication using mode division multiplexing (MDM)[1-3] has been actively studied to overcome the capacity crunch caused by the rapid growth of the internet traffic. In the MDM systems, independent time series signal is modulated to each of a plurality of spatial modes. A selective launching of spatial modes into multi-mode fibers (MMF), one of the key technologies for MDM, can be realized with free-space optics by use of phase plates[4, 5] or spatial light modulators (SLM)[6-8]. The use of phase plates has much simple scheme, while generated spatial modes have long tail components which are not included in the ideal spatial modes. This is because that this method modulates only spatial phase distribution of an incident light. Specifically, these components often cause the modal cross-talk. In contrast, displaying computer generated holograms (CGH) on a SLM, in which original complex object is encoded as amplitude or phase hologram through interference with a plane wave[9], offers us methods for constructing arbitrary complex fields with high accuracy. However, the modulated light by CGH methods includes not only desired diffraction order but also unwanted diffraction orders. This causes the significantly degradation of the light utilization efficiency.

To overcome this problem, we propose a spatial mode generation technology using a spatial cross modulation (SCM) method[10]. In the SCM, the complex amplitude field of the desirable spatial mode is computationally encoded into a scattered phase-only image by the light scattering with a virtual random diffuser. Then, the phase conjugated image of the diffused image is displayed onto a phase-only SLM (PSLM). After modulating the incident light by the PSLM, the spatial mode is reconstructed by making the modulated light pass through an actual random diffuser in order to cancel the random phase modulation. In this way, the SCM can reconstruct the desired complex amplitude with high accuracy and greater light utilization efficiency than that of the CGH methods.

*sakuma@optnet.ist.hokudai.ac.jp; phone 81 11 706-6522; fax 81 11 706-7836

Next-Generation Optical Communication: Components, Sub-Systems, and Systems V,
edited by Guifang Li, Xiang Zhou, Proc. of SPIE Vol. 9774, 97740K · © 2016 SPIE
CCC code: 0277-786X/16/$18 · doi: 10.1117/12.2211948

In Sect. 2, we describe the basic principle of our technology. In Sect. 3, we perform a numerical simulation to verify that our technology can be applied for the spatial mode generation technology. In this simulation, we use two-dimensional (2D) fast-Fourier transform (FFT) and inverse FFT (IFFT) for the calculation of light wave propagation. Sequentially, we make a comparison between our technology and the technology using an off-axis amplitude hologram based on the two viewpoints: the accuracy and the optical power loss. In Sect. 4, we perform an experiment on spatial modes generation using the SCM with the PSLM and the optical random diffuser. Finally, the conclusion is given in Sect. 5.

2. SPATIAL MODE GENERATION USING SPATIAL CROSS MODULATION

The conceptual diagram of the spatial mode generation technology using SCM is shown in Fig. 1. The basic operation of our technology is divided into two steps: the calculation of the scattered wavefront (encode step) and the reconstruction of the complex amplitude field (decode step). These two steps are illustrated as Fig. 1(a) and Fig. 1(b), respectively. The encode step is virtually performed within a computer. In contrast, the decode step is performed by an actual optical system.

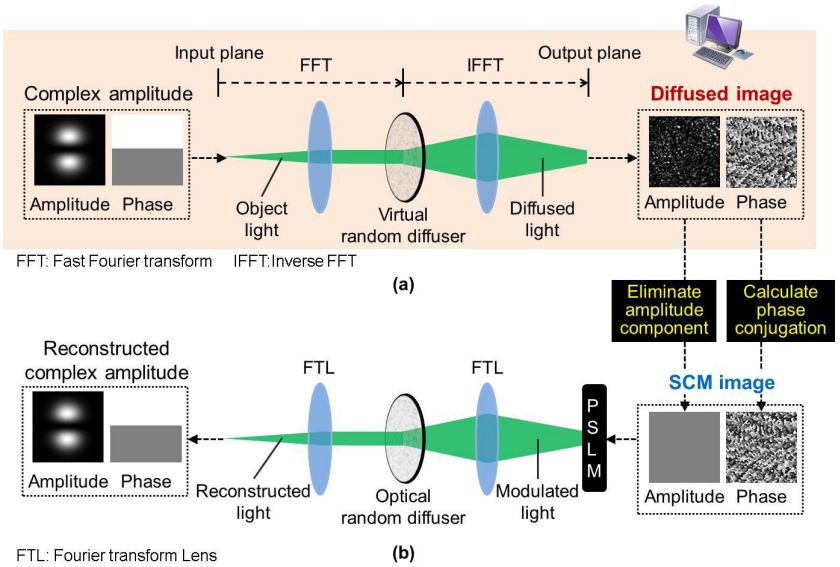

Figure 1. Conceptual diagram of a spatial mode generation technology using a spatial cross modulation method. (a) Encode step performed within the computer. (b) Decode step performed by the actual optical system.

In the encode step, a complex amplitude $A(x,y)\exp[j\varphi(x,y)]$ of desired spatial modes is firstly prepared in an input plane. Next, the spatial spectrum of the complex amplitude $F\{A(x,y)\exp[j\varphi(x,y)]\}$ is calculated by Fourier-transformation with FFT and multiplied with the phase distribution of a virtual random diffuser $\exp[jh_{vir}(x,y)]$. Here, $F\{\cdot\}$ denotes the operator of 2D Fourier transform. After that, a diffused image of the original complex amplitude $S(x,y)\exp[j\xi(x,y)]$ is obtained on the output plane by inverse Fourier-transformation with IFFT. Subsequently, the amplitude distribution in the diffused image $S(x,y)$ are uniformized. This operation is based on the fact that the phase part in a homogeneous scattered light contains most of the important features of the original complex object. This importance of phase has been demonstrated in a number of different studies, including optical and acoustical holograms[11, 12]. Finally, the phase conjugated image $\exp[-j\xi(x,y)]$ is calculated to be used in the following decode step. Herein, the phase-only diffused image $\exp[-j\xi(x,y)]$ is referred to as the SCM image.

In the decode step, the SCM image is firstly displayed onto a PSLM. After incident light falls on the PSLM, the modulated light $\exp[-j\xi(x,y)]$ is Fourier-transformed $F\{\exp[-j\xi(x,y)]\}$ via the first lens. Then, the light was transmitted through the optical random diffuser whose phase distribution is $\exp[jh_{opt}(x,y)]$. Since random phase distribution modulated by the virtual random diffuser is canceled, the reconstructed object $A'(x,y)\exp[j\varphi'(x,y)]$ is obtained by passing through the second lens. Note that the reconstructed object $A'(x,y)\exp[j\varphi'(x,y)]$ is extremely similar to the original object $A(x,y)\exp[j\varphi(x,y)]$, but the random noise slightly occurs due to the elimination of the scattered amplitude distribution. Here, phase distributions of the virtual random diffuser $\exp[jh_{vir}(x,y)]$ and that of the optical random diffuser $\exp[jh_{opt}(x,y)]$ must be matched for correctly working the SCM. Two approaches for matching these phase distributions

can be considered. In the first approach, the phase distribution of the optical random diffuser used for decode step is measured in advance and the measured phase distribution is used for the virtual diffuser in the encode step. In the second approach, the random phase distribution used for the encode step is displayed onto the PSLM which is used as the optical random diffuser.

In the off-axis CGH, the desired complex amplitude field is obtained with first order diffraction light and only extracted with a spatial filtering. This causes significant decrease of the light utilization efficiency. On the other hand, in SCM, desired complex field is provided with zeroth order diffraction light. Hence, our technology can achieve lager light utilization efficiency than that of the technology using the off-axis CGH.

3. SIMULATION

3.1 Models and flows

We perform a numerical simulation to make a comparison between our technology and the technology using, as a representative CGH method, an off-axis amplitude hologram. In the following, the off-axis amplitude hologram is referred to as the off-axis CGH. The simulation models of our technology and the off-axis CGH are illustrated in Fig. 2. Simulation parameters are summarized in Table 1. In this simulation, five types of linearly polarized (LP) modes (LP_{01}, LP_{11}, LP_{21}, LP_{51}, LP_{101}) are prepared for a desired complex object, as shown in Fig. 3. For the calculation of light wave propagation, 2D FFT and IFFT are used. In the SCM, a complex object light is multiplied by the random diffuser, and then a diffused image is obtained in output plane (Step 1~Step 5). After that, the amplitude distribution is uniformized (Step 6), and the SCM image is calculated by phase conjugation of the diffused image (Step 7). Next, the SCM image is displayed onto a SLM, and plane wave irradiates the SLM (Step 8). Finally, after the modulated light is retransmitted through the optical random diffuser, the reconstructed light is obtained in fiber input plane (Step 9~Step 12). In the case of off-axis CGH, a complex object light is collimated and interfered with an off-axis reference plane wave (Step 1~Step3). Then, its interferogram is displayed onto the SLM, and the reference light is irradiated (Step4). Finally, the reconstructed light is obtained in fiber input plane via the lens (Step 5, Step 6).

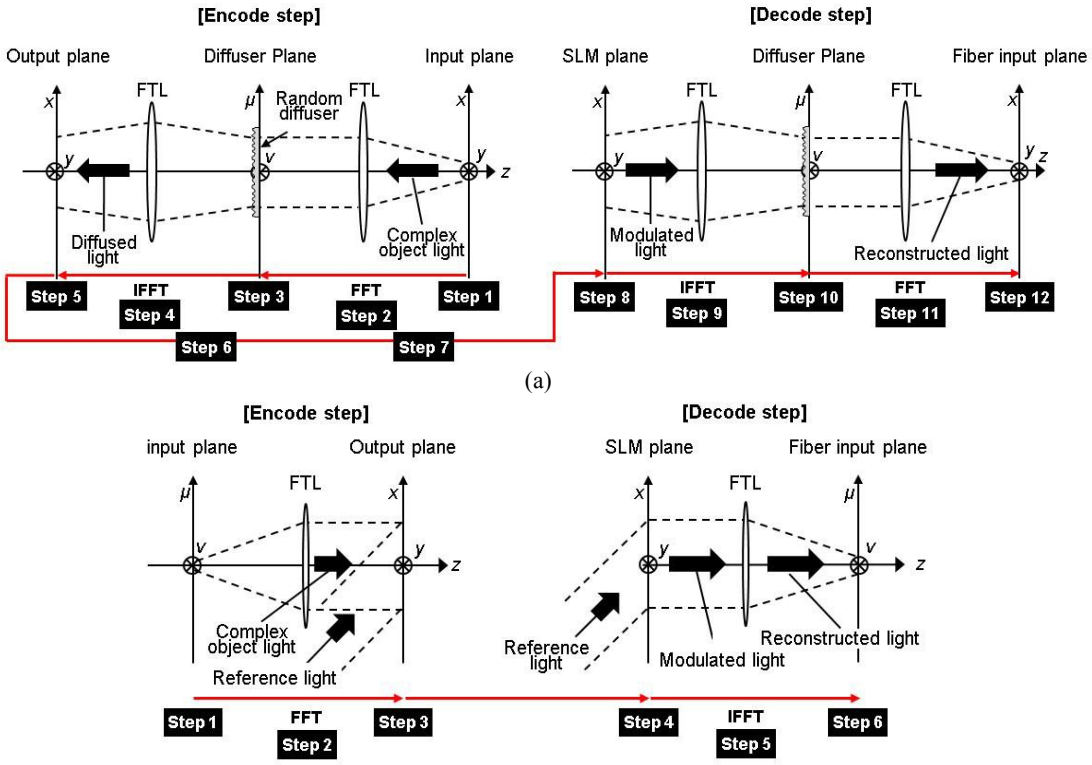

Figure 2. Simulation models of (a) spatial cross modulation and (b) off-axis CGH. In the off-axis CGH, unwanted diffraction orders are omitted.

Table 1. Simulation parameters.

Common parameters		Parameters for SCM	
Wavelength of laser source, λ (nm)	1300	Diffusion angle of diffuser, θ_{diff} (degree)	42.0
Number of data pixels, $N_{dx} \times N_{dy}$	1024 × 1024	Gray level of diffuser, G_{diff} (level)	2048
Size of data pixels, $P_{dx} \times P_{dy}$ (μm^2)	1.0	Refractive index of diffuser, n_{diff}	1.5
Zero padding rate, N_0	2		
Parameters for LP modes		**Parameters for off-axis CGH**	
Core diameter, d_{core} (μm)	62.5	Incident angle of reference light, θ_{in} (degree)	15.0
Core index, n_{core}	1.46		
Relative index difference, Δ	0.01		

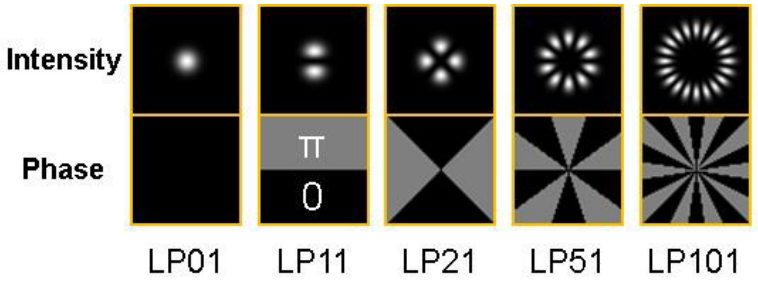

Fig. 3. Intensity and phase distributions of LP modes for an input complex object.

3.2 Results

For making a comparison between our technology using and the technology using the off-axis CGH, we evaluate the results from two points of the accuracy and the optical power loss.

First, the evaluation in terms of the accuracy of the reconstructed complex amplitude distribution is performed. A coupling efficiency (CE) η is used as an indicator of the accuracy of reconstructed modes. The CE between the reconstructed mode and desirable $LP_{\mu,v}$ mode is calculated as

$$\eta_{\mu,v} = \left| \iint E_{rec}(x,y) \cdot E^{*}_{\mu,v}(x,y)\, dxdy \right|^2 , \quad (1)$$

where * denotes the complex conjugation, $E_{rec}(x,y)$ and $E_{\mu,v}(x,y)$ denotes the reconstructed mode and desirable $LP_{\mu,v}$ mode, respectively. The integration range is set to the core diameter. The higher CE indicates that the reconstructed complex amplitude distribution is closer to the desirable LP mode. In other words, the reconstructed complex field can transmits more energy into the desirable LP mode. Figure 4(a) shows the CE of each reconstructed LP mode. As shown in Fig 4(a), the CE of the off-axis CGH achieves great value of over -0.02 dB, and then the CE of the SCM is lower through all LP modes. However, the SCM also achieves very high CE of over -0.12 dB. We can consider that these deteriorations of the CE are caused by slight random noise which is occurred due to the elimination of the scattered amplitude information in the encode step.

Another comparison in terms of the optical power loss is performed by the evaluation of the light utilization efficiency (LUE). Here, the LUE is defined as the power ratio of the reconstructed light into the region of the fiber core to the incident light into the optical system. Figure 4(b) shows the LUE of each reconstructed LP mode. The CE of the off-axis CGH rises with increasing the order of LP modes but maintains a still very low value of less than -14.6 dB. This order dependence of the CE is caused owing to that the focal length of each lens is fixed. To overcome this problem, the modification of the optical system or additional dynamic optical elements is required. In contrast, the SCM keeps great LUE of over -2.2 dB at any order. Moreover, our technology is hardly dependent on the order of LP modes.

Finally, we can consider that the power ratio of the light coupled into the desired LP mode to the incident light into the optical system from the product of the CE and LUE. In this regard, we can see that our technology overwhelms the technology using the off-axis CGH. Consequently, it is clear that the SCM has great potential to realize a spatial mode generation technology for MDM with high accuracy and large light utilization efficiency.

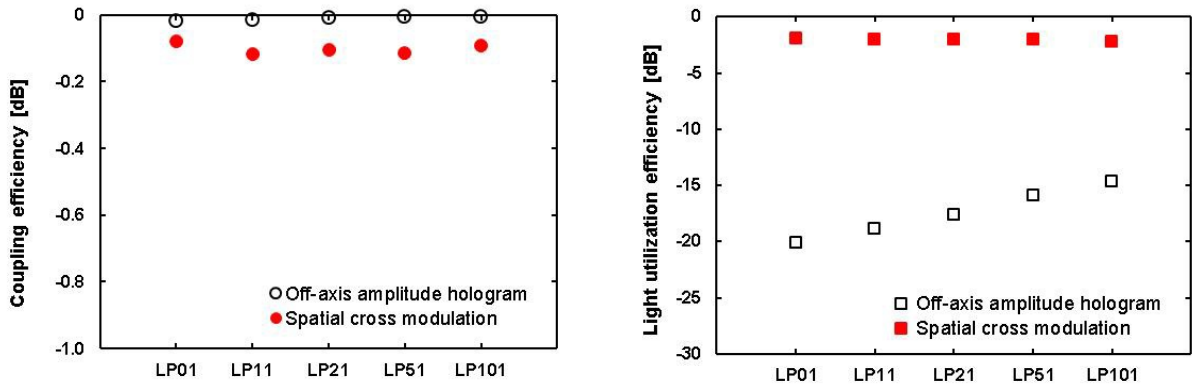

(a) (b)

Figure 4. Comparison of simulation results between the SCM and the off-axis CGH. (a) Coupling efficiency. (b) Light utilization efficiency.

4. EXPERIMENT

4.1 Experimental setup

Experimental setup is shown in Fig. 5. In this section, we performed an experiment on the reconstruction of complex amplitude distributions of spatial modes in Object plane instead of Fourier plane. This is because that a commercially available PSLM does not have sufficient small pixel size. The SCM was implemented with an optical random diffuser whose phase distribution was previously measured. We prepared five types of LP modes (LP_{01}, LP_{11}, LP_{21}, LP_{51}, LP_{101}) as input complex object. The original complex amplitude that has the number of data pixels of 200 × 200 was diffused and encoded into the SLM pixels of 400 × 400. Then, the SCM image was displayed onto the PSLM. After that, the complex amplitude distribution of the reconstructed light was measured by holographic diversity interferometry (HDI) [13, 14], which is one of the phase-shifting digital holography.

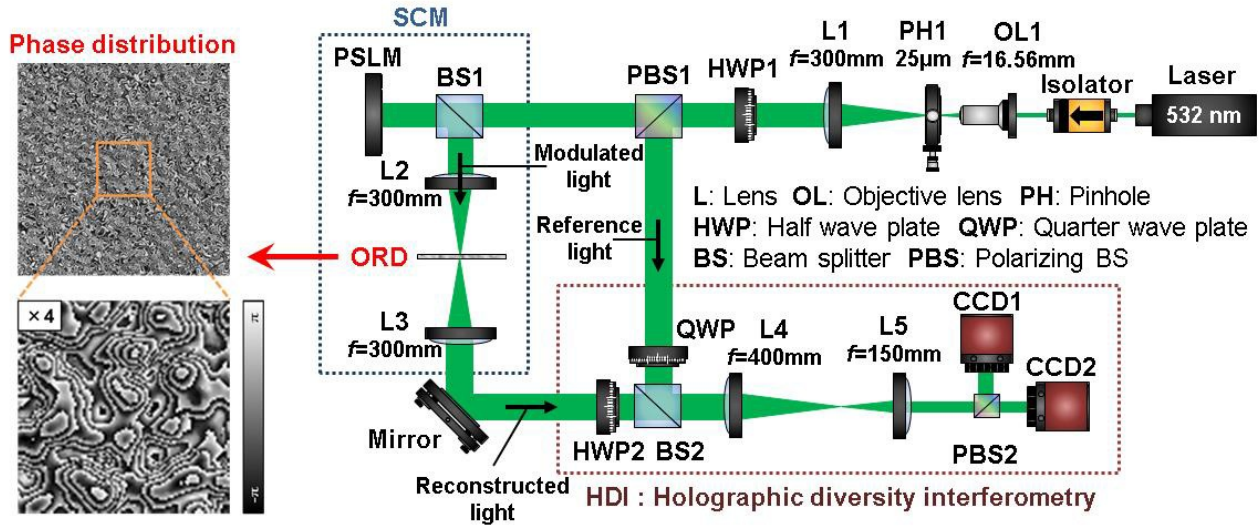

Figure 5. Experimental setup. The wavelength is 532 nm. The PSLM (Hamamatsu, x1222-01) has pixel size of 20 × 20 μ m^2 and the pixel number of 800 × 600. CCDs (Stingray, F125B) have the pixel size of 3.75 × 3.75 μm^2 and the pixel number of 1280 × 960. Optical random diffuser (Edmund, #48-012) has the diffusion angle of 0.5 °.

4.2 Results

Figure 6 shows the experimental results. We can see that intensity and phase distribution of the measured complex amplitude is similar to desirable LP mode at LP_{01}, LP_{11}, LP_{21} and LP_{51}. Although the phase distribution of the measured complex amplitude at LP_{101} corresponds to the desirable LP mode, the intensity distribution is significantly degraded.

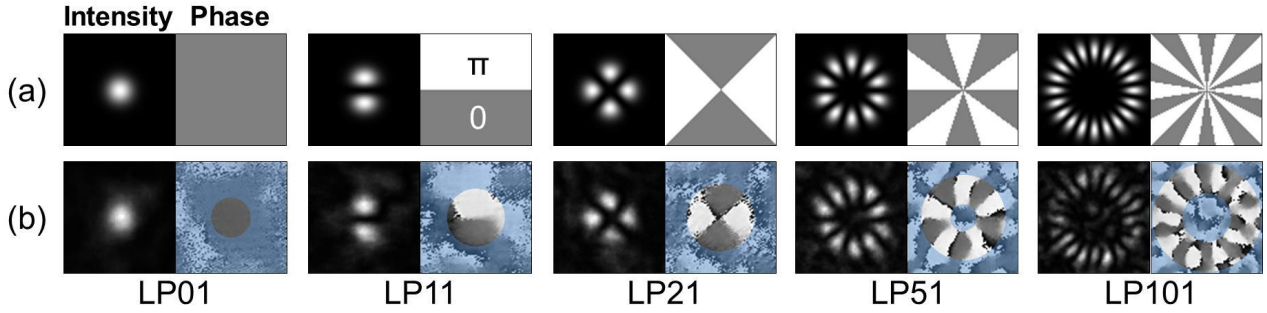

Figure 6. Experimental results. Intensity and phase distribution of (a) desirable LP modes and (b) measured complex amplitude field. The blue-colored areas in the phase parts of measured complex amplitude correspond to the indefinite areas for phase values on the desirable LP modes.

We evaluated the CE between the measured complex amplitude distribution and the complex amplitude distribution in object plane of the desirable LP mode, as shown in Fig. 7. In Fig. 7, the CE maintains low value less than -1.2 dB through all LP modes.

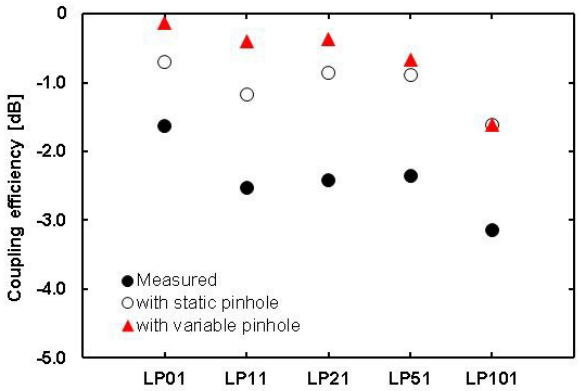

Figure 7. Coupling efficiency in Object plane. ●: Measured complex amplitude. ○: Complex amplitude filtered by static pinhole within the computer. ▲: Complex amplitude filtered by variable pinhole within the computer. The size of aperture of the static pinhole and the variable pinhole are optimized for the CE of LP101 and the CE of each LP mode, respectively.

As the main factor causes these deteriorations, we can consider that the diffusion angle of the optical random diffuser or the number of pixels of the PSLM is insufficient. In the experiment, the optical random diffuser that has the comparatively low diffusion angle of 0.5° was employed due to the restriction on the spatial resolution of the phase measurement. The diffusion angle is critical parameter for our technology because the SCM utilize the importance of phase in scattered wavefront. Insufficient of the number of SLM pixels also can be considered as another factor. In this experiment, pixel matching between the PSLM and CCDs restricts us to use a part of the whole SLM pixels. Actually, the previous study on the SCM[10] reported that the reproduction quality of the SCM depends on the diffusion angle and the ratio of the original and encoded image seizes. Next, we put a static pinhole or a variable pinhole in a computer to minimize the influence of noise components occurred by that random phase modulation is not completely canceled out with the optical random diffuser. From Fig. 7, it is confirmed that the random phase modulation remaining in the reconstructed light strongly decreases the CE. We expect that our technology can achieve great CE without any spatial filtering by using a wider-spreading optical random diffuser and an enough high-resolution SLM because it enhances the fidelity of complex amplitude field of the reconstructed light at diffuser plane and therefore suppresses the influence of residual random phase modulation.

5. CONCLUSION

We proposed a new spatial mode generation technology using the SCM for MDM. First, we performed a numerical simulation to verify that the SCM is applicable for spatial modes generation technology. In this simulation, five types LP modes (LP_{01}, LP_{11}, LP_{21}, LP_{51} and LP_{101}) were prepared for the input complex object. Then, we made a comparison in terms of the coupling efficiency and the light utilization efficiency between our technology and the technology using the off-axis amplitude hologram. Simulation results revealed that the SCM can achieve comparable high CE of over -0.12 dB and large LUE of over -2.2 dB through all modes without modification of an optical system and dynamic optical elements. Next, we demonstrated the spatial mode generation using our technology with a substitute optical system. In the experiment, complex amplitude distributions in object plane of LP modes were reconstructed. Experimental results showed that although a spatial filtering is required, our technology can achieve the CE of over -0.7 dB at LP_{01}, LP_{11}, LP_{21} and LP_{51}. We expect that our technology using a wider-spreading optical random diffuser and an enough high-resolution SLM enables us to improve the accuracy without any modification of the optical system and additional dynamic optical elements.

ACKNOWLEDGMENT

This work was supported by KAKENHI (25289110).

REFERENCES

[1] Berdagué, S. and Facq, P., "Mode division multiplexing in optical fibers," Appl. Opt 21(11), 1950-1955 (1982).
[2] Ryf, R., Randel, S., Gnauck, A. H., Bolle, C., Sierra, A., Mumtaz, S., Esmaeelpour, M., Burrows, E. C., Essiambre, R.-J., Winzer, P. J., Peckham, D. W., McCurdy, A. H. and Lingle, R., "Mode-division multiplexing over 96 km of few-mode fiber using coherent 6 × 6 MIMO processing," J. Lightwave Technol. 30(4), 521-531 (2012).
[3] Okamoto, A., Morita, K., Wakayama, Y., Tanaka, J. and Sato, K., "Mode division multiplex communication technology based on dynamic volume hologram and phase conjugation," Proc. SPIE 7716, 771627 (2010).
[4] Thornburg, W. Q., Corrado, B. J. and Zhu, X. D., "Selective launching of higher-order modes into an optical fiber with an optical phase shifter," Opt. Lett. 19(7), 454-456 (1994).
[5] Mohammed, W., Pitchumani, M., Metha, A. and Johnson, E. G., "Selective excitation of the LP_{11} mode in step index fiber using a phase mask," Opt. Eng. 45(7), 074602 (2006).
[6] Stepniak, G., Maksymiuk, L. and Siuzdak, J., "Binary-phase spatial light filters for mode-Selective excitation of multimode fibers," J. Lightwave Technol. 29(13), 1980-1987 (2011).
[7] von Hoyningen-Huene, J., Ryf, R. and Winzer, P., "LCoS-based mode shaper for few-mode fiber," Opt. Express 21(15), 18097-18110 (2013).
[8] Okamoto, A., Aoki, K., Wakayama, Y., Soma, D. and Oda, T., "Multi-excitation of spatial modes using single spatial light modulator for mode division multiplexing," Proc. OFC2012, JW2A.38 (2012).
[9] Arizzón, V., Méndez, G. and Sánchez-de-La-Llave, D., "Accurate encoding of arbitrary complex fields with amplitude-only liquid crystal spatial light modulators," Opt. Express 13(20), 7913-7927 (2005).
[10] Shibukawa, A., Okamoto, A., Takabayashi, M. and Tomita, A., "Spatial cross modulation method using a random diffuser and phase-only spatial light modulator for constructing arbitrary complex fields," Opt. Express 22(4), 3968-3982 (2014).
[11] Oppenheim, A. V. and Lim, J. S., "The importance of phase in signals," Proc. IEEE 69(5), 529-541 (1981).
[12] Horner, J. L. and Gianino, P. D., "Phase-only matched filtering," Appl. Opt. 23(6), 812-816 (1984).
[13] Okamoto, A., Kunori, K., Takabayashi, M., Tomita, A. and Sato, K., "Holographic diversity interferometry for optical storage," Opt. Express 19(14), 13436-13444 (2011).
[14] Nozawa, J., Okamoto, A., Shibukawa, A., Takabayashi, M. and Tomita, A., "Two-channel algorithm for single-shot, high-resolution measurement of optical wavefronts using two image sensors," Appl. Opt. 54(29), 8644-8652 (2015).